Medicinal Chemistry Research
https://doi.org/10.1007/s00044-018-2271-0

MEDICINAL CHEMISTRY RESEARCH

ORIGINAL RESEARCH

Novel anti-cancer agents: design, synthesis, biological activity, molecular docking, and MD simulations of 2, 3, 4, 5-tetrahydro-1*H*-pyrido-[4,3-b]indole derivatives

Yu Feng[1] · Xingxing Teng[1] · Jinhua Gu[1] · Bangwei Yu[2] · Yan Luo[1] · Lianbao Ye[1,3]

Received: 27 March 2018 / Accepted: 4 December 2018

Abstract

In the previous research, our group designed and synthesized 2,3,4,5-tetrahydro-1*H*-pyrido-[4,3-b] indoles, which showed high anti-tumor activity. In this study, a series of novel 2,3,4,5-tetrahydro-1*H*-pyrido-[4,3-b] indole derivatives were designed by introducing an alkyl or aralkyl and a sulfonyl group, which are considered as the pharmacophores of some antitumor drugs based on the combination principles, and synthesized. The antiproliferative activity of all the target compounds were evaluated against Hela, A549, HepG2, and MCF-7 cell lines using the MTT assay in vitro. The results were represented by IC_{50} values. All compounds showed moderate to excellent antiproliferative activity with IC_{50} values between 0 μM and 100 μM against cancer cells. The proliferations of Hela, A549, HepG2, and MCF-7 cell lines were inhibited in a dose-dependent manner, and the cytolytic activity was markedly inhibited at the same time. The IC_{50} values of intermediate **3** inhibited against Hela, A549, HepG2, and MCF-7 cell lines were 52.75, 50.30, 60.31, and 54.39 μM, respectively, which were higher than the new compounds that we expected. The compounds **4a**–**4d** bearing sulfonyl, substituted by electron donating group, showed moderate to significant antiproliferative activity, in which compound **4c** was the best with the IC_{50} values of 13.71, 9.42, 15.06, and 14.77 μM, and these results suggested that the introduction of sulfonyl could increase the antiproliferative activity of 2,3,4,5-tetrahydro-1*H*-pyrido-[4,3-b]indole. Compounds **4e**–**4g** bearing alkyl, phenyl, and arylated alkyl produced good antiproliferative activity and the IC_{50} value of **4g** was lower than 30 μM. The target compounds were more potent against A549 compared to the other three cell lines. Molecular docking studies revealed the binding orientations of all the synthesized compounds in the active site of c-Met. Moreover, molecular dynamics simulations have been performed to evaluate the binding stabilities between the synthesized compounds and their receptors.

Keywords 2,3,4,5-Tetrahydro-1*H*-pyrido-[4,3-b]indole derivatives · Design and synthesis · Biological activities · Molecular docking · Molecular dynamics simulations

Introduction

Finding the effective and specific anti-tumor drug has epoch-making significance since malignant tumor is a serious threat to human health. There are plenty of studies on the treatment of cancer by chemotherapeutic agents that can act directly on DNA or interfere with the

Supplementary information The online version of this article (https://doi.org/10.1007/s00044-018-2271-0) contains supplementary material, which is available to authorized users.

✉ Lianbao Ye
yelb7909@163.com

[1] School of Pharmacy, Guangdong Pharmaceutical University, 510006 Guangzhou, China

[2] Institute of Traditional Chinese Medicine, Guangdong Pharmaceutical University, 510006 Guangzhou, China

[3] Key Laboratory of New Drug Discovery and Evaluation of Ordinary Universities of Guangdong Province, Guangzhou Key Laboratory of Construction and Application of New Drug Screening Model Systems, Guangzhou Key Laboratory of Construction and Application of New Drug Screening Model Systems and Guangdong Province Engineering Technology Center for Molecular Probes & Biomedical Imaging, Guangdong Pharmaceutical University, Guangzhou, 510006 Guangdong, China

Published online: 14 December 2018

synthesis of DNAs to inhibit the proliferation and metastasis of tumor cells (Johnson 2000; Lee et al. 2014; Bellacosa et al. 2013). Tumor-targeting therapies have significantly changed cancer treatments, which depend on specific vectors to kill the tumor cells so as to improve the efficacy and reduce the toxic side effects on normal cells (Kircheis et al. 2002; Hofmeister et al. 2008). In the previous research, our group designed and synthesized a new compound **1** (Fig. 1) bearing active skeleton 2,3,4,5-tetrahydro-1*H*-pyrido-[4,3-b]indole, which showed high antiproliferative activity and c-Met inhibitory potency (Ye et al. 2012). Additionally, molecular docking studies showed that the main binding mode of 2,3,4,5-tetrahydro-1*H*-pyrido-[4,3-b]indole with c-Met kinase site was the hydrophobic region (Ye et al. 2016). In an ongoing effort to discover novel anti-tumor agents, we were going to design and synthesize novel 2,3,4,5-tetrahydro-1*H*-pyrido-[4,3-b]indoles using compound **1** as the leading compound based on combination principles.

Related references reported that the sulfonamide group was the pharmacophore of some anti-tumor drugs. Natural products such as coumarins, in which a sulfonamide group was introduced, have antiproliferative activity (Bhat et al. 2006; Luo et al. 2001; Farahi et al. 2015; Kovác et al. 2001; Thaisrivongs et al. 1994; Dang et al. 2010; Chandak et al., 2016; Desai et al. 2014). The sulfonamide group has substituted for structurally similar amino sulfonic esters, and has shown well antiproliferative activity in vivo and in vitro according to the biological isostere principles. Additionally, we expected that bearing an alkyl or aralkyl in position N-5 would both be absorbed by various tissues quickly and increase the antiproliferative activity. Our group reported that a series of small molecule inhibitors of c-Met, which are prepared by sulfonic acids and natural products, inhibited the proliferation of many tumor cell lines excellently (Ye et al. 2017). It is hoped that the introduction of sulfonyl, alkyl, or aralkyl (Fig. 2) can increase the antiproliferative activity of 2,3,4,5-tetrahydro-1*H*-pyrido-[4,3-b]indole. Hopefully, it was quickly and effectively absorbed by the creased polarity and increased the lipid solubility.

In this study, all compounds synthesized were evaluated for their antiproliferative activity in vitro against Hela, A549, HepG2, and MCF-7 cells. In addition, molecular docking study simulated the interaction between small molecule ligands and receptor macromolecules at the molecular level. Molecular dynamics (MD) experiments were performed to evaluate the binding stabilities between the compounds and their receptors.

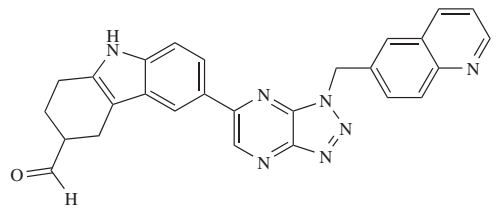

Fig. 1 Structure of **1**

Fig. 2 Target compounds

General Structure	Compound	R
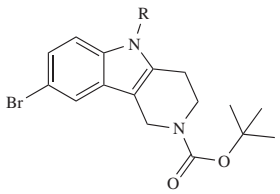	**4a**	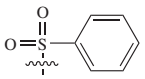
	4b	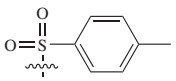
	4c	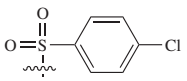
	4d	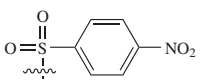
	4e	
	4f	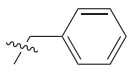
	4g	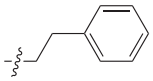

Material and methods

Unless otherwise noted, all the chemicals were obtained from Aladdin or J&K Scientific Ltd., China. The solvents were purified and dried based on standard procedures and stored over 3A molecular sieves. The reactions progress was determined by thin layer chromatography (TLC) analysis on silica gel F_{254} plate (Merck). Chromatography purification was run on silica gel (200–300 mesh) from Qingdao Ocean Chemical (Qingdao, Shandong, China). ^{1}H NMR and ^{13}C NMR spectra were recorded on a Bruker Digital NMR Spectrometer, rep, δ (ppm), J in Hz, using tetramethylsilane (TMS) as an internal standard and $CDCl_3$ or DMSO-d_6 as solvent. The chemical structures of the target compounds were determined by Electron Impact Mass Spectra (EI-MS) using a Waters ZQ400 instrument. RPMI-1640 culture medium and new-born calf serum were purchased from Gibco (Grand Island, NY), and methyl thiazolyl tetrazolium (MTT) was purchased from Amresco (Solon, OH).

Synthesis of compounds

Synthesis of 2

4-Bromophenylhydrazine hydrochloride (224 mg, 1 mmol) and *N*-tert-butoxycarbonyl-4-piperidone (298.5 mg, 1.5 mmol) were dissolved in 10 ml ethanol solution and saturated hydrochloric acid, and the mixture was stirred at 95 °C for 8 h. The solution was filtered; the filtered cake was rinsed with anhydrous ethanol and dried in vacuo to give **2** (151 mg, 60%) as a white solid.

Synthesis of 3

The compound **2** (251 mg, 1 mmol) and di-tert butyl dicarbonate (262 mg, 1.2 mmol) were dissolved in dichloromethane (8 ml). Then *N*, *N*-disopropylamine (268 mg, 2 mmol) was added slowly under stirring. The solution was poured into H_2O, and extracted with dichloromethane, then dried over anhydrous sodium sulfate, filtered, and evaporated. The crude product was purified by column chromatography (dichloromethane/methanol, 23/1) to give **3** (299 mg, 88.9%) as a faint yellow solid.

Synthesis of 4a

The compound **3** (351 mg, 1 mmol), $(Bu_4N)_2SO_4$ (50 wt%, solution in H_2O, 0.4 ml), and 6 N NaOH solution (0.32 ml) were dissolved in toluene (8 ml) under an ice bath and stirred for 15 min. Benzenesulfonyl chloride (176 mg, 1 mmol) was added slowly. The mixture was vigorously stirred for 2.5 h at r.t. under nitrogen. The solution was poured into H_2O and ethyl acetate was added to the suspension, dried over anhydrous sodium sulfate, filtered, and evaporated. The crude product was purified by column chromatography (petroleum ether/ethyl acetate, 10/4), to afford the compound (393 mg, 78%) as a yellow solid.

Synthesis of 4b–4d

Compounds were prepared in analogy to **4a**.

Synthesis of 4e

To a solution of **3** (351 mg, 1 mmol) in N,N-Dimethylformamide (DMF) (8 ml) at 0 °C under N_2, sodium hydride (60% weight dispersion in mineral oil) was added, the mixture was stirred at 0 °C for 30 min. Methyl iodide (284 mg, 2 mmol) was added, and the reaction mixture was stirred overnight at ambient temperature, quenched by adding a saturated solution of ammonium chloride. The mixture was extracted three times with equivalent dichloromethane and the combined extracts dried over sodium sulfate. After concentration in vacuum, the residue was purified by column chromatography (petroleum ether/ethyl acetate, 10:4) to obtain the product (223 mg, 61%) as a yellow solid.

Synthesis of 4f–4g

Compounds were prepared in analogy to **4e**.

Cell assay

The anti-proliferative activities of compounds **4a**–**4g** were evaluated against Hela, A549, HepG2, and MCF-7 cell lines using the standard MTT assay in vitro. The cancer cell lines were cultured in minimum essential medium (DMEM) supplemented with 10% fetal bovine serum (FBS) and 100 μg ml^{-1} penicillin. Approximately 1.0×10^4 cells ml^{-1} with 200 μl of DMEM medium were plated onto each well of a 96-well plate and incubated in 5% CO_2 at 37 °C for 24 h. The target products at indicated final concentrations (0–800 μM) or 0.1% Dimethyl sulfoxide (DMSO) were added to the medium for 24 and 48 h. Fresh MTT (10 μl) was added to each well and at a terminal concentration of 5 μg ml^{-1} and incubated with the cells at 37 °C in dark for 4 h. The formazan crystals were dissolved in 100 μl of DMSO in each well and shaken for 15 min to dissolve it completely. The absorbance at 492 nm was measured with a SpectraMAX190 micro plate reader (Molecular Devices, USA). All target products were tested three times in each of the cell lines. The results expressed as IC_{50} (inhibitory concentration 50%) were the averages of three determinations and were calculated by using the GraphPad Prism 5 software.

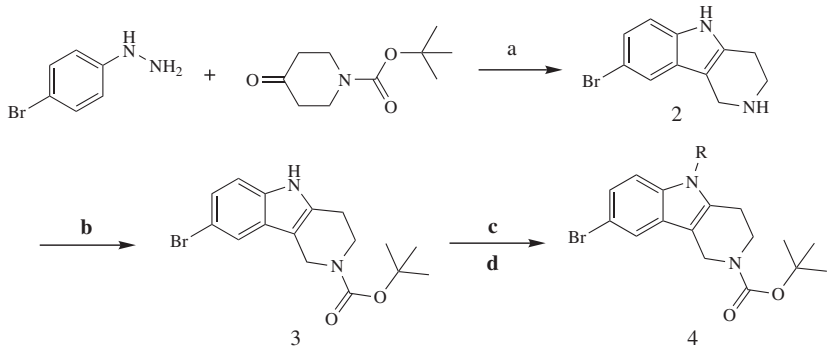

Fig. 3 Synthesis of compounds, reagents, and conditions: **a** EtOH/HCl, 90 °C, 8 h; **b** DIEA, DCM, rt, 5 h; **c** $(Bu4N)_2SO_4$, 6 N NaOH, toluene, rt, 4 h; **d** NaH, DMF, rt, overnight

Molecular docking

Molecular docking was performed according to the related references (Pirali et al. 2010; Huang et al. 2013; Ye et al. 2015). To further elucidate the binding mode of compounds in the tyrosine kinase ligand binding region, the CDOKER program which connected with Accelrys Discovery Studio 2.5.5 was used to simulate. CDOKER can offer all the advantages of full ligand flexibility (including bonds, angels, and dihedrals), the CHARMm family of force field, the flexibility of CHARMm engine, and reasonable computation times, which has an important advantage of introducing the soft-core potentials. In this work, we maintained the root-mean-square deviation (RMSD) value of the optimum pose less than 1Å of the related crystal pose and optimized the crystal structure of 3EFJ with polar hydrogen atoms and CHARMm force field, but not water. We set the radius of the input site sphere as 10 Å from the center of the binding site, and each ligand generated 20 random conformations. The ligands' other parameters were default values. The optimized ligands were docked into the corresponding proteins active binding site according to the protocol. The structure of the receptor was minimized to 10,000 cycles using the Powell method in DS2.5.5. The convergence criterion was identified as 0.001 kcal mol^{-1}.

MD simulations

MD is a general simulation technique that is included in many molecular modeling packages such as CHARMm and AMBER. Applying MD to evaluate the binding stabilities between all the compounds and the 3EFJ due to the possible binding mode, which was predicted by molecular docking studies between a ligand and receptor, may be not reasonable or stable (Tian et al. 2014; Yuan et al. 2014; Hou et al. 2012; Yan et al., 2016; He et al. 2010). In this work, we used AMBER 10.0 for ligands and AMBER ff03 for proteins on the basis of molecular docking results. The Gaussian 0.3 program was used to calculate partial atomic charges of the ligand by using the HF/6-31G* basis set and the Antechamber module was used to fit the restricted electrostatic potential (RESP).The simulations were performed at a neutral pH and the hydrogen bonds were constrained using SHAKE algorithm. The residue-based cut-off 10 Å was used for nonbonded interaction and the time step was set to 2 fs. The G-quadruplex complex and inner ions were initially fixed with force constants of 100 kcal mol^{-1}. The system was heated from 0 to 300 K in 100 ps with solutes constrained at a weak harmonic constraint of 10 kcal mol^{-1} and then equilibrated for 100 ps after all the minimization steps contained 2000 cycles of steepest descent minimization, followed by 2000 cycles of conjugated gradient minimization. Finally, periodic boundary dynamics simulations of 8 ns were carried out in an NPT ensemble at 1 atm and 300 K in the production step. The output trajectory files were saved every 2 ps for subsequent analysis.

Results and discussion

Chemistry

The synthesis of the key intermediate of tert-butyl-8-bromo-2, 3,4,5-tetrahydro-1*H*-pyrido-[4,3-b]indole carboxylate was achieved according to previous reported general procedure using commercially available 4-bromophenylhydrazine hydrochloride and *N*-tert-butoxycarbonyl-4-piperidone as starting materials based on Fischer Indolizations (Fig. 3). Different benzene sulfonyl groups were added to the N of 9-position of tert-butyl-8-bromo-2,3,4,5-tetra-hydro-1*H*-pyrido-[4,3-b]indole carboxylate to obtain tert-butyl-8-bromo-5-(phenyl-sulfonyl)-3,4-dihydro-1*H*-pyrido-[4,3-b]indole-2-carboxylate (**4a**), tert-butyl-8-bromo-5-tosyl-3,4-dihydro-1*H*-pyrido-[4,3-b]indole-2-carboxylate (**4b**), tert-butyl-8-bromo-5-[(4-chlorophenyl)sulfonyl]-3,4-dihydro-1*H*-pyrido-[4,3-b]indole-2-carboxylate (**4c**), tert-butyl-8-bromo-5-[(4-nitro-phenyl)sulfonyl]-3,4-dihydro-1*H*-pyrido-[4,3-b]indole-2-carboxylate (**4d**) via nucleophilic substitution with yields of 63%, 61%, 58%, and 52%, respectively. This reaction provided good yields using sodium hydroxide as a catalyst and $(Bu_4N)_2SO_4$ as a phase transfer catalyst and the reaction was completed within 10 h due to the hydrolysis of sulfonyl

chloride when it was treated with water. Benzene sulfochloride substituted by electron donating group would obtain high yield. Furthermore, the compounds tert-butyl-8-bromo-5-methyl-3,4-dihydro-1*H*-pyrido-[4,3-b]indole-2-carboxylate(**4e**), tert-butyl-8-bromo-5-benzyl-3,4-dihydro-1*H*-pyrido-[4,3-b]indole-2-carboxylate (**4f**), and tert-butyl-8-bromo-5-phenethyl-3,4-dihydro-1*H*-pyrido-[4,3-b]indole-2-carbo-xylate (**4g**) were synthesized with yields of 69%, 63%, 61%, respectively. Sodium hydride was used as a strong base to make a compound alkylated by deprotonation and *N*, *N*-dimethylformamide was used as a solvent.

8-Bromo-2,3,4,5-tetrahydro-1*H*-pyrido-[4,3-b]indole (2)

Yield: 60%, ^{1}H NMR (400 MHz, $CDCl_3$) δ 7.38 (s, 1H), 7.20 (dd, $J = 8.2$, 1.3 Hz, 1H), 6.98 (dd, $J = 8.2$, 1.3 Hz, 1H), 3.65 (s, 2H), 3.00 (m, 4H). ^{13}C NMR (100 MHz, (D_6) DMSO) δ 136.35 (C-5), 131.91 (C-8), 126.74 (C-4), 123.58 (C-1), 121.75 (C-3), 113.79 (C-2), 113.10 (C-6), 107.82 (C-7), 44.43 (C-10), 43.09 (C-12), 25.68 (C-13). EI-MS: 251.33 [M+H$^+$]. Anal. calcd. for $C_{11}H_{11}BrN_2$(250.01): C, 52.61; H, 4.42; Br, 31.82; N, 11.16. Found: C, 52.59; H, 4.42; Br, 31.81; N, 11.13.

Tert-butyl-8-bromo-2,3,4,5-tetrahydro-1*H*-pyrido-[4,3-b] indole carboxylate (3)

Yield: 78%, ^{1}H NMR (400 MHz, $CDCl_3$) δ 7.39 (t, $J = 1.6$ Hz, 1H), 7.20 (dd, $J = 8.2$, 1.6 Hz, 1H), 6.98 (dd, $J = 8.1$, 1.5 Hz, 1H), 4.49 (s, 2H), 3.70 (dd, $J = 9.6$, 4.7 Hz, 2H), 3.07 (dd, 2H), 1.41 (s, 9H). ^{13}C NMR (100 MHz, (D_6) DMSO) δ 154.69 (C-15), 136.35 (C-5), 131.91 (C-8), 126.74 (C-4), 123.58 (C-1), 121.75 (C-3), 113.79 (C-2), 113.10 (C-6), 107.82 (C-7), 81.41 (C-17), 51.11 (C-10), 49.57 (C-12), 28.22 (C-18, C-19, C-20), 23.21 (C-13). EI-MS: 351.24 [M+H$^+$]. Anal. calcd. for $C_{16}H_{19}BrN_2O_2$ (350.06): C, 54.71; H, 5.45; Br, 22.75; N, 7.98; O, 9.11. Found: C, 54.70; H, 5.45; Br, 22.73; N, 7.99; O, 9.10.

Tert-butyl-8-bromo-5-(phenylsulfonyl)-3,4-dihydro-1*H*-pyrido-[4,3-b]indole-2-carboxylate (4a)

Yield: 63%, ^{1}H NMR (400 MHz, $CDCl_3$) δ 8.44 (dd, $J =$ 4.5, 1.5 Hz, 1H), 7.82 (dd, $J = 8.1$ Hz, 2H), 7.74 (t, $J = 7.7$ Hz, 1H), 7.50 (t, $J = 7.7$ Hz, 2H), 7.36 (dd, J = 8.3, 1.8 Hz, 1H), 7.21 (dd, J = 8.4, 4.7 Hz, 1H), 3.76 (t, J = 5.1 Hz, 2H), 3.31–3.13 (m, 2H), 1.37 (s, 9H). ^{13}C NMR (100 MHz, (D_6) DMSO) δ 154.69 (C-15), 139.96 (C-8), 137.86 (C-25), 135.96 (C-5), 131.46 (C-28), 129.17 (C-27, C-29), 126.80 (C-26, C-30), 121.75 (C-3), 114.98 (C-6), 113.79 (C-2), 107.82 (C-7), 81.41 (C-17), 51.11 (C-10), 49.57 (C-12), 28.22 (C-18, C-19, C-20), 25.68 (C-13). EI-MS: 491.40 [M +H$^+$]. Anal. calcd. for $C_{22}H_{23}BrN_2O_4S$ (490.06): C, 53.77; H, 4.72; Br, 16.26; N, 5.70; O, 13.02; S, 6.52. Found: C, 53.73; H, 4.70; Br, 16.23; N, 5.70; O, 13.00; S, 6.49.

Tert-butyl-8-bromo-5-tosyl-3,4-dihydro-1*H*-pyrido-[4,3-b] indole-2-carboxylate (4b)

Yield: 61%, ^{1}H NMR (400 MHz, $CDCl_3$) δ 8.44 (dd, $J = 4.5$, 1.8 Hz, 1H), 7.58 (dd, $J = 7.8$ Hz, 2H), 7.36 (dd, $J = 8.4$, 1.6 Hz, 1H), 7.30 (d, $J = 7.6$ Hz, 2H), 7.21 (dd, $J = 8.5$, 4.7 Hz, 1H), 4.77 (s, 2H), 3.76 (t, $J = 5.1$ Hz, 2H), 3.27–3.15 (m, 2H), 2.47 (s, 3H), 1.37 (s, 9H).^{13}C NMR (100 MHz, (D_6) DMSO) δ 154.69 (C-15), 144.28 (C-31), 139.96 (C-8), 135.96 (C-5), 135.00 (C-25), 129.42 (C-27, C-29), 127.11 (C-26, C-30), 121.75 (C-3), 114.98 (C-6), 113.79 (C-2), 107.82 (C-7), 81.41 (C-17), 51.11 (C-10), 49.57 (C-12), 28.22 (C-18, C-19, C-20), 25.68 (C-13), 21.27 (C-31). EI-MS: 505.43 [M +H$^+$]. Anal. calcd. for $C_{23}H_{25}BrN_2O_4S$ (504.07): C, 54.66; H, 4.99; Br, 15.81; N, 5.54; O, 12.66; S, 6.34. Found: C, 54.64; H, 4.99; Br, 15.80; N, 5.52; O, 12.65; S, 6.31.

Tert-butyl-8-bromo-5-[(4-chlorophenyl)sulfonyl]-3,4-dihydro-1*H*-pyrido-[4,3-b]indole-2-carboxylate (4c)

Yield: 58%, ^{1}H NMR (400 MHz, $CDCl_3$) δ 8.43 (dd, $J = 4.4$, 1.6 Hz, 1H), 7.71 (dd, $J = 7.9$ Hz, 2H), 7.58 (dd, $J = 7.9$ Hz, 2H), 7.35 (dd, $J = 8.3$, 1.5 Hz, 1H), 7.20 (dd, $J = 8.5$, 4.4 Hz, 1H), 4.75 (s, 2H), 3.76 (t, $J = 5.1$ Hz, 2H), 3.29–3.13 (m, 2H), 1.37 (s, 9H). ^{13}C NMR (100 MHz, (D_6) DMSO) δ 154.69 (C-15), 154.69 (C-8), 139.96 (C-5), 135.18 (C-28), 130.01 (C-27, C-29), 129.12 (C-1), 128.37 (C-26, C-30), 126.74 (C-4), 121.75 (C-3), 114.98 (C-6), 113.79 (C-2), 107.82 (C-7), 81.41 (C-17), 51.11 (C-10), 49.57 (C-12), 28.22 (C-18, C-19, C-20), 25.68 (C-13). EI-MS: 525.84 [M +H$^+$]. Anal. calcd. for $C_{22}H_{22}BrClN_2O_4S$ (524.02): C, 53.88; H, 4.52; Br, 16.29; N, 5.71; O, 13.05; S, 6.54. Found: C, 53.87; H, 4.50; Br, 16.30; Cl, 6.02; N, 5.70; O, 13.03; S, 6.54.

Tert-butyl-8-bromo-5-[(4-nitrophenyl)sulfonyl]-3,4-dihydro-1*H*-pyrido-[4,3-b]indole-2-carboxylate (4d)

Yield: 52%, ^{1}H NMR (400 MHz, $CDCl_3$) δ 8.45 (dd, $J =$ 4.7, 1.6 Hz, 1H), 8.22 (dd, 1H), 8.07 (dd, $J = 7.9$, 3.7 Hz, 2H), 7.37 (dd, $J = 8.3$, 1.8 Hz, 1H), 7.21 (dd, $J = 8.3$, 4.6 Hz, 1H), 4.80 (s, 2H), 3.76 (t, $J = 5.0$ Hz, 2H), 3.21 (t, 2H), 1.37 (s, 9H). ^{13}C NMR (100 MHz, (D_6) DMSO) δ 154.69 (C-5), 140.48 (C-28), 139.96 (C-8), 135.96 (C-5), 135.11 (C-25), 129.12 (C-1), 128.57 (C-26, C-30), 126.74 (C-4), 121.75 (C-3), 117.31 (C-27, C-29), 114.98 (C-6), 113.79 (C-2), 107.82 (C-7), 81.41 (C-17), 51.11 (C-10), 49.57 (C-12), 28.22 (C-18, C-19, C-20), 25.68 (C-13). EI-MS: 536.40 [M +H$^+$]. Anal. calcd. for $C_{22}H_{22}BrN_3O_6S$ (535.04): C, 49.26; H, 4.13; Br, 14.90; N, 7.83; O, 17.90; S, 5.98. Found: C, 49.24; H, 4.11; Br, 14.89; N, 7.83; O, 17.88; S, 5.97.

Table 1 IC_{50} values of all compounds against Hela, A549, HepG2, and MCF-7 cell lines in vitro

Compound	Hela IC_{50} (μM) ± SD		A549 IC_{50} (μM) ± SD		HepG2 IC_{50} (μM) ± SD		MCF-7 IC_{50} (μM) ± SD	
	24 h	48 h	24 h	48 h	24 h	48 h	24 h	48 h
2	57.21 ± 0.40	60.00 ± 0.52	54.28 ± 0.49	59.27 ± 0.36	62.37 ± 0.47	69.13 ± 0.40	57.72 ± 0.38	68.36 ± 0.60
3	52.75 ± 0.35	56.21 ± 0.41	50.3 ± 0.28	56.18 ± 0.31	60.31 ± 0.47	63.77 ± 0.49	54.39 ± 0.29	62.9 ± 0.40
4a	47.21 ± 0.56	49.89 ± 0.27	38.72 ± 0.16	40.61 ± 0.19	46.88 ± 0.43	49.49 ± 0.27	42.5 ± 0.37	49.72 ± 0.29
4b	19.6 ± 0.27	20.64 ± 0.20	17.03 ± 0.11	17.92 ± 0.15	20.01 ± 0.16	22.8 ± 0.10	19.63 ± 0.19	19.01 ± 0.13
4c	13.71 ± 0.15	13.5 ± 0.09	9.42 ± 0.08	8.3 ± 0.07	15.06 ± 0.14	15.81 ± 0.20	14.77 ± 0.08	17.91 ± 0.17
4d	29.1 ± 0.21	30.51 ± 0.27	25.06 ± 0.15	25.74 ± 0.22	30.61 ± 0.27	32.04 ± 0.31	20.99 ± 0.16	21.7 ± 0.11
4e	38.99 ± 0.31	38.72 ± 0.24	31.73 ± 0.19	33.05 ± 0.22	31.97 ± 0.40	35.69 ± 0.19	30.65 ± 0.24	33.08 ± 0.52
4f	28.01 ± 0.28	29.99 ± 0.17	26.14 ± 0.33	26.03 ± 0.28	30.58 ± 0.24	33.18 ± 0.49	29.5 ± 0.15	31.27 ± 0.32
4g	20.97 ± 0.18	23.62 ± 0.22	18.4 ± 0.10	19.33 ± 0.21	21.6 ± 0.14	25.01 ± 0.21	18.27 ± 0.19	20.51 ± 0.16

Tert-butyl-8-bromo-5-methyl-3,4-dihydro-1*H*-pyrido-[4,3-b] indole-2-carboxylate (4e)

Yield: 69%, ^{1}H NMR (400 MHz, $CDCl_3$) δ 7.40 (dd, J = 7.9, 2.2 Hz, 1H), 7.27 (t, J = 1.9 Hz, 1H), 6.81 (dd, J = 8.1, 1.8 Hz, 1H), 4.50 (s, 2H), 3.74 (s, 3H), 3.66 (t, J = 5.1 Hz, 2H), 3.20–3.06 (m, 2H), 1.41 (s, 9H). ^{13}C NMR (100 MHz, (D_6) DMSO) δ 154.69 (C-15), 136.37 (C-5),131.34 (C-1), 126.74 (C-4), 121.75 (C-3), 116.21 (C-6), 113.79 (C-2), 107.82 (C-7), 81.41 (C-17) 51.11 (C-10), 49.57 (C-12), 31.40 (C-22), 28.22 (C-18, C-19, C-20), 25.68 (C-13). EI-MS: 365.27 [M+H$^+$]. Anal. calcd. for $C_{17}H21_{Br}N_2O_2$ (364.06): C, 55.90; H, 5.80; Br, 21.88; N, 7.67; O, 8.76. Found: C, 55.93; H, 5.79; Br, 21.89; N, 7.67; O, 8.74.

Tert-butyl-8-bromo-5-benzyl-3,4-dihydro-1*H*-pyrido-[4,3-b] indole-2-carbox-ylate (4f)

Yield: 63%, ^{1}H NMR (400 MHz, $CDCl_3$) δ 7.25 (ddd, J = 11.1, 10.5, 5.8 Hz, 4H), 6.94 (m, 2H), 6.83 (d, J = 8.1 Hz, 1H), 5.23 (s, 2H), 4.53 (s, 2H), 3.62 (t, J = 5.5 Hz, 2H), 3.13 (t, 2H), 1.39 (s, 9H). ^{13}C NMR (100 MHz, (D_6) DMSO) δ 154.69 (C-15), 136.85 (C-23), 136.31 (C-5), 136.16 (C-8), 131.34 (C-1), 128.94 (C-26), 128.60 (C-25, C-27), 127.99 (C-24, C-28), 126.74 (C-4), 121.75 (C-3), 116.21 (C-6), 113.79 (C-2), 107.82 (C-7), 81.41 (C-17), 51.11 (C-10), 49.57 (C-12), 47.01 (C-22), 28.22 (C-18, C-19, C-20), 25.68 (C-13). EI-MS: 441.37 [M+H$^+$]. Anal. calcd. for $C_{23}H_{25}BrN_2O_2$ (440.11): C, 62.59; H, 5.71; Br, 18.10; N, 6.35; O, 7.25. Found, C, 62.58; H, 5.72; Br, 18.08; N, 6.33; O, 7.26.

Tert-butyl-8-bromo-5-phenethyl-3,4-dihydro-1*H*-pyrido-[4,3-b]indole-2-car-boxylate (4g)

Yield: 61%, ^{1}H NMR (400 MHz, $CDCl_3$) δ 7.25 (ddd, J = 8.1, 6.0, 2.6 Hz, 3H), 7.21–7.16 (m, 1H), 7.15–7.06 (m, 1H), 6.82 (d, J = 8.1 Hz, 1H), 4.56 (s, 2H), 4.26 (t, J = 7.4 Hz, 2H), 3.62 (t, 2H), 3.33 (t, J = 7.4 Hz, 2H), 3.13 (t, J = 4.43 Hz, 2H), 1.39 (s, 9H). ^{13}C NMR (100 MHz, (D_6) DMSO) δ 154.69 (C-15), 138.68 (C-24), 136.31 (C-5), 136.16 (C-8), 131.34 (C-1), 128.94 (C-27), 128.72 (C-26, C-28), 128.49 (C-25, C-29), 126.74 (C-4), 121.75 (C-3), 116.21 (C-6), 113.79 (C-2), 107.82 (C-7), 81.41 (C-17), 51.11 (C-10), 49.57 (C-12), 35.70 (C-23), 28.22 (C-18, C-19, C-20), 25.68 (C-13). EI-MS: 455.40 [M+H$^+$]. Anal. calcd. for $C_{24}H_{27}BrN_2O_2$ (454.13): C, 63.30; H, 5.98; Br, 17.55; N, 6.15; O, 7.03. Found: C, 63.28; H, 5.99; Br, 17.56; N, 6.17; O, 7.01.

Evaluation of the biological activity

The antiproliferative activity of all the target compounds was evaluated against Hela, A549, HepG2, and MCF-7 cell lines using the MTT assay in vitro.The results were represented by IC_{50} values as shown in Table 1. The IC_{50} values were obtained by at least three independent trials. All compounds showed moderate to excellent antiproliferative activity with IC_{50} values between 0 μM and 100 μM against cancer cells as illustrated in Fig. 4. The proliferations of Hela, A549, HepG2, and MCF-7 cell lines were inhibited in a dose-dependent manner, and the cytolytic activity was markedly inhibited at the same time. Moreover, there was no significant difference between the inhibitory effects of the all compounds on the growth of the tumor cells for 24 h and 48 h; thus, there was no significant influence on the antiproliferation effect of compounds on Hela cells, A549 cells, HepG2 cells, and MCF-7 cells with an extended treatment time after 24 h. The IC_{50} values of intermediate **3** inhibited against Hela, A549, HepG2, and MCF-7 cell lines were 52.75, 50.30, 60.31, 54.39 μM, respectively, which were higher than the new compounds that we expected. The compounds **4a**–**4d** bearing sulfonyl, which was substituted by the electron donating group, showed moderate to significant antiproliferative activity, in which compound **4c** was the best with the IC_{50} values of 13.71, 9.42, 15.06,

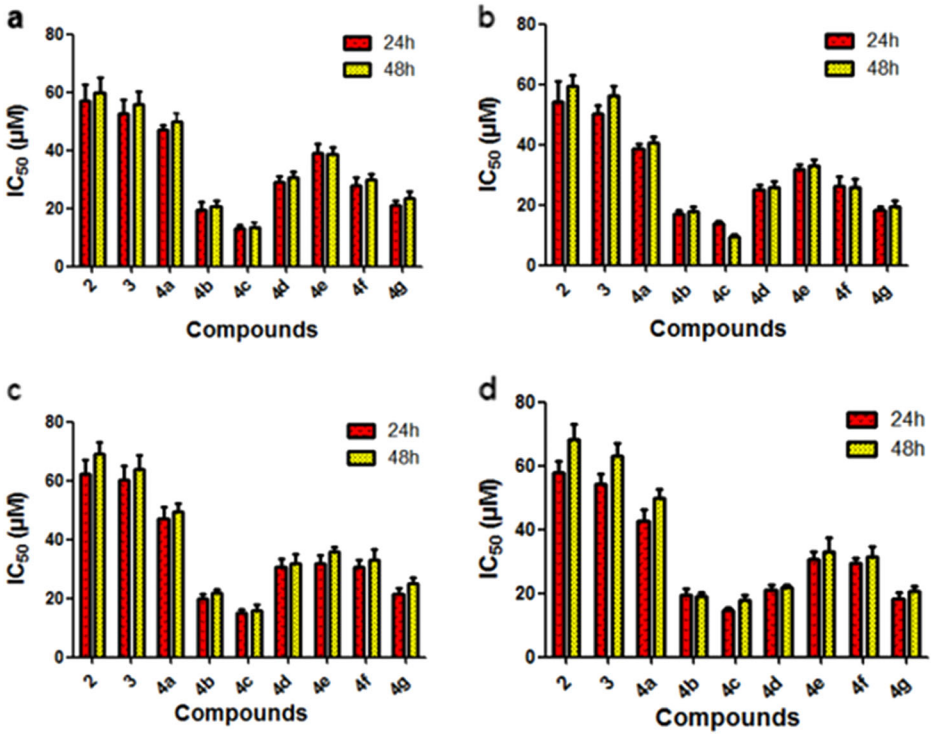

Fig. 4 The inhibition of all compounds on Hela **a**, A549 **b**, HepG2 **c**, and MCF-7 **d** cells

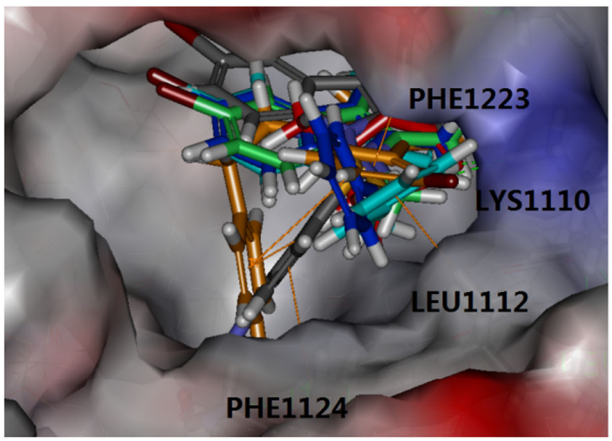

Fig. 5 Compact binding modes of all compounds (PDB:3EFJ)

14.77 μM, and these results suggested that the introduction of sulfonyl group could increase the antiproliferative activity of 2,3,4,5-tetrahydro-1*H*-pyrido-[4,3-b]indole. Compounds **4e**–**4g** bearing alkyl, phenyl, and arylated alkyl groups produced good antiproliferative activity and the IC_{50} value of **4g** was lower than 30 μM. In general, the target compounds were more potent against A549 compared to the other three cell lines. In addition, DMSO alone did not show obvious inhibitory effect compared to untreated cells. These results revealed that this series of compounds possessed selectivity for A549 cancer cell lines, and had the makings of good drugs for lung cancer. Based on the molecular docking, MD simulations, and preliminary activity tests, we could initially confirm that the target compounds might well repay investigation. In conclusion, the compounds synthesized by our experimental scheme had a good inhibitory effect on cancer cells, and they could be used as the leading compounds for the development of new anticancer inhibitors, and this study was of great significance to the establishment of the chemical library and further research studies.

Molecular docking

In pre-experiment, we carried out the docking experiment by using several pdb proteins including 3DKF, 3EFJ, 3F82, 3WGJ, and 3RTO. Only 3EFJ interacted with compound **2**; compound **3** and derivatives achieved good binding effect owing to the stable indole fused ring structure, so we chose it for the docking experiment. The 3EFJ is the crystal structure of c-Met kinase in complex with ATP and its information is seen from http://www.rcsb.org/pdb/explore/explore.do?structureId=3EFJ.

Molecular docking suggested that these compounds were bound to the active site of the protein 3EFJ (shown in Fig. 5). Docking experiments were performed to elucidate the binding model of the strongest compounds **4c** with c-Met kinase, as shown in Fig. 6. Compound **4c** was docked into the binding site of c-Met kinase using CDOCKER (dock ligands into an active site using CHARMm) program conducted through Discovery Studio 2.5.5. The docking experiments suggested that compound **4c** would dock

strongly into the ATP-binding site of c-Met. The binding energies of complexes between all compounds and 3EFJ are shown in Table 2. The strong interaction of **4c** with c-Met was attributed to two H-bonds between two oxygen atoms on the sulfonyl group and THR1257 and GLN1256; in addition, there was also a H-bond between the chlorine atom and hydroxyl of THR1293. The π–π stacking interaction between the indole ring and the benzene sulfonyl would make the binding more firm between small **4c** and 3EFJ. Moreover, **4c** showed highest activity owing to the π–π stacking interaction between the pyrrole ring and phenyl of indole and PHE1223, H-bond between carbonyl oxygen and GLN1258. Thus, it was illustrated that the compounds **4a–4d**, bearing a benzene ring substituted by the electron donating group, showed higher binding energies and compounds **4e–4g**, bearing arylated alkyl, produced the highest activity.

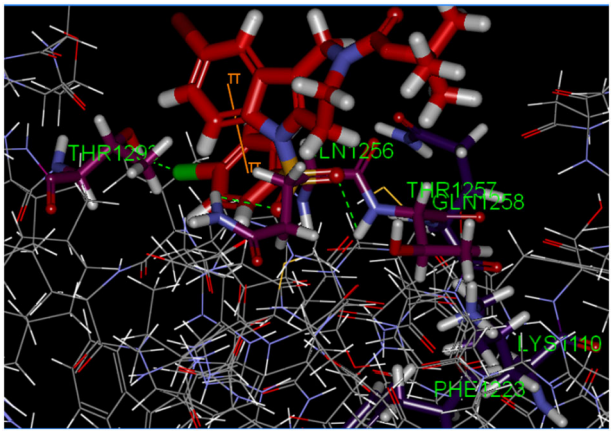

Fig. 6 Docking model of compounds **4c** (red) with c-Met (3EFJ)

MD simulations

Molecular docking studies were first carried out to predict the plausible interactions between all compounds and 3EFJ. On the basis of the docking results, MD simulation may provide information on rearrangement and transition states. The crystal structures of 3EFJ complex with compounds **2**, **3**, and **4a–4g** were used to evaluate the reliability of MD simulations. As a result, the MD models appeared to reach a stable state after 1 ns equilibration and the RMSD values converged below 2.5 Å, especially the binding state between **4c** and 3EFJ was relatively stable and the trajectories were smooth (Fig. 7). The MD parameters we chose were appropriate for the MD simulations.

Most compounds gave stable RMSD curves during their simulations (shown in Fig. 8). The binding free energies ΔGpred were computed by means of MM-PBSA inside the Amber 10 program, where values more negative than −20 kcal mol^{-1} were selected to assess the inhibitory activity for

Table 2 Binding energies of complexes between all compounds and 3EFJ

Compounds	R	-CDOCKER energy (kcal mol^{-1})
2	_	21.8334
3	-Boc	25.7259
4a		32.2177
4b		53.7629
4c		59.4801
4d	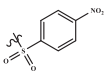	40.6372
4e		44.8160
4f		47.0279
4g		48.9527

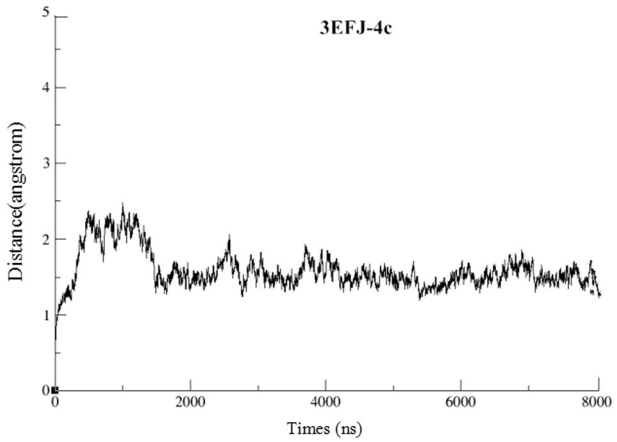

Fig. 7 Plot of RMSD for all the backbond atoms (Å) vs simulation time (ns) for 3EFJ in complex with **4c**

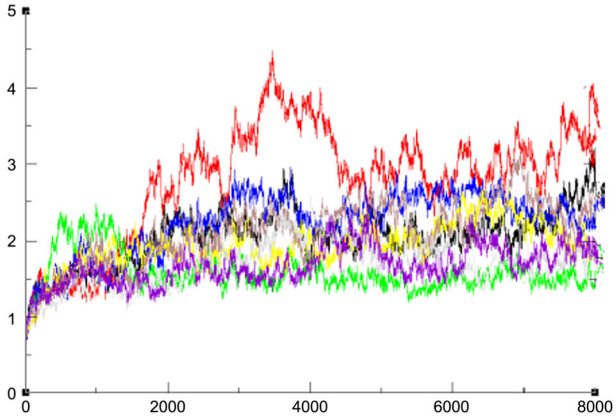

Fig. 8 Plot of RMSD for all the backbond atoms (Å) vs simulation time (ns) for 3EFJ in complex with compounds **4a**–**4g**

Table 3 Predicted binding free energies (ΔGpred, kcal mol^{-1}) of **2**–**4g** inhibitors selected for the bioassay

Compound	R	ΔGpred	std
2	_	-11.48	±2.86
3	-Boc	-15.62	±2.51
4a		-16.94	±3.04
4b		-26.81	±3.10
4c		-30.75	±2.73
4d		-21.06	±2.09
4e		-20.96	±2.81
4f		23.83	±3.17
4g		-23.75	±2.95

3EFJ. The predicted ΔGpred values of all compounds are listed in Table 3.

MM-PBSA estimation of binding free energy ΔGpred

For each system, the values were calculated using 100 snapshots recorded from the last with 1 ns trajectory at an interval of 10 ps by Molecular Mechanics Poisson–Boltzmann Surface Area method.

Acknowledgements The work was supported by the Special Innovation Project of Guangdong Education Department (Natural Science) (2017KTSCX107), Guangdong Natural Science Foundation (2015A03031356), Science and Technology Planning Project of Guangdong Province (2017ZC0199), Guangdong Provincial Applied Scientific and Technological Project (2015B020234009), National Scientific and Technological Project of Traditional Chinese Medicine Industry (201507004), Guangdong Pharmaceutical University' School Powered by Innovation Foundation of China (2016KZDXM039), and Guangdong special training fund for university students' scientific and technological innovation (51328004). The authors are grateful to Mr. Tan and Sun Yet-Sen University for molecular docking experiment.

Compliance with ethical standards

Conflict of interest The authors declare that they have no conflict of interest.

References

Bellacosa A, Yen T, Beeharry N, Smith M (2013) Combination of DNA repair inhibition with bendamustine or gemcitabine in the treatment of cancer. US Patent 2013-0303588, filled 15 Mar 2013, issued 6 Jan 2015

Bhat M, Siddiqui N, Khan S (2006) Synthesis of novel thioureido derivatives of sulfonamides and thiosemicarbazido derivatives of coumarin as potential anticonvulsant and analgesic agents. Indian J Pharm Sci 68:120

Chandak N, Ceruso M, Supuran CT, Sharma PK (2016) Novel sulfonamide bearing scaffolds as selective inhibitors of tumor associated carbonic anhydrase isoforms IX and XII. Bioorg Med Chem 24:2882–2886

Dang YY, Li XC, Zhang QW, Li SP, Wang YT (2010) Preparative isolation and purification of six volatile compounds from essential oil of Curcuma wenyujin using high-performance centrifugal partition chromatography. J Sep Sci 33:1658–1664

Desai NC, Satodiya HM, Rajpara KM, Joshi VV, Vaghani HV (2014) ChemInform abstract: microwave assisted synthesis of new coumarin based 3-cyanopyridine scaffolds bearing sulfonamide group having antimicrobial activity. ChemInform 45:904–914

Farahi M, Karami B, Tanuraghaj HM (2015) ChemInform abstract: efficient synthesis of a new class of sulfonamide-substituted coumarins. Tetrahedron Lett 56:1833–1836

He L, He F, Bi H, Li J, Zeng S, Luo HB, Huang M (2010) Isoform-selective inhibition of chrysin towards human cytochrome P450 1A2. Kinetics analysis, molecular docking, and molecular dynamics simulations. Bioorg Med Chem Lett 20:6008–6012

Hofmeister V, Schrama D, Becker JC (2008) Anti-cancer therapies targeting the tumor stroma. Cancer Immunol Immunother 57:1–17

Hou JQ, Chen SB, Tan JH, Luo HB, Li D, Gu LQ, Huang ZS (2012) New insights from molecular dynamic simulation studies of the multiple binding modes of a ligand with G-quadruplex DNA. J Comput Aided Mol Des 26:1355–1368

Huang YY, Li Z, Cai YH, Feng LJ, Wu Y (2013) The molecular basis for the selectivity of tadalafil toward phosphodiesterase 5 and 6: a modeling study. J Chem Inf Model 53:3044

Johnson DH (2000) Evolution of cisplatin-based chemotherapy in non-small cell lung cancer: a historical perspective and The Eastern Cooperative Oncology Group experience. Chest 117:133S–137S

Kovác M, Sabatié A, Floch L (2001) Synthesis of coumarin sulfonamides and sulfonylurea. Arkivoc 6:100–108

Kircheis R, Wightman L, Kursa M, Ostermann E, Wagner E (2002) Tumor-targeted gene delivery: an attractive strategy to use highly active effector molecules in cancer treatment. Gene Ther 9:731–735

Lee TC, Su TL, Chon TC (2014) Method of treating cancer using combination of a bifunctional alkylating agent and DNA repair inhibitors. US Patent 8772284, filled 27 Oct 2010, issued 8 July 2014

Luo X, Xiu N, Cheng L, Huang D (2001) Synthesis of coumarin dyes containing N -alkylsulfonamide groups. Dyes Pigm 51:153–159

Pirali T, Faccio V, Mossetti R, Grolla AA, Di Micco S, Bifulco G, Genazzani AA, Tron GC (2010) Synthesis, molecular docking and biological evaluation as HDAC inhibitors of cyclopeptide mimetics by a tandem three-component reaction and intramolecular [3+2] cycloaddition. Mol Divers 14:109–121

Thaisrivongs S, Tomich PK, Watenpaugh KD, Chong KT, Howe WJ, Yang CP, Strohbach JW, Turner SR, McGrath JP, Bohanon MJ (1994) Structure-based design of novel HIV protease inhibitors: sulfonamide-containing 4-hydroxycoumarins and 4-hydroxy-2-pyrones as potent non-peptidic inhibitors. J Med Chem 37:3200–3204

Tian Y, Shen Y, Zhang X, Ye L, Li Z, Liu Z, Zhang J, Wu S (2014) Design some new type I c-met inhibitors based on molecular docking and topomer CoMFA research. Mol Inform 33:536

Ye L, Tian Y, Li Z, Zhang J, Wu S (2012) Design and synthesis of some novel 2,3,4,5-tetra hydro -1H-pyrido [4,3-b]indoles as potential c-Met inhibitors. Helv Chim Acta 95:320–326

Ye L, Wu J, Yang J, Chen W, Luo L, Zhang Y (2016) Biological activity, molecular docking studies and molecular dynamics simulations of 2,3,4,5-tetrahydro-1H-pyrido[4,3-b] indoles as c-Met inhibitors. Lat Am J Pharm 35:416–420

Ye L, Wu J, Chen W, Feng Y, Shen Z (2017) Novel anti-cancer agents based on germacrone: design, synthesis, biological activity, docking studies and MD simulations. RSC Adv 7:3760–3767

Ye L, Wu J, Yang J, Chen W, Luo Y, Zhang Y (2015) Design, synthesis and molecular docking analysis of some novel 7-[(quinolin-6-yl) methyl] purines as potential c-Met inhibitors. Med Chem Res 24:3327–3333

Yuan H, Zhuang J, Hu S, Li H, Xu J, Hu Y, Xiong X, Chen Y, Lu T (2014) Molecular modeling of exquisitely selective c-Met inhibitors through 3D-QSAR and molecular dynamics simulations. J Chem Inf Model 54:2544

Yan M, Wang H, Wang Q, Zhang Z, Zhang C (2016) Allosteric inhibition of c-Met kinase in sub-microsecond molecular dynamics simulations induced by its inhibitor Tivantinib. Phys Chem Chem Phys 18:10367–10374